

Multi-objective optimizations of mechanical characteristics of objects in computer aided SIS manufacturing process using empirical PSO algorithm

Mohammed YUNUS, Mohammad S. ALSOUFI

Mechanical Engineering Department, College of Engineering and Islamic Architecture, Umm Al-Qura University, Abidiah, Makkah, Kingdom of Saudi Arabia

myhasan@uqu.sa, m.s.alsoufi@gmail.com

Abstract: Implementation of the “Selective Inhibition type of Sintering (SIS)” method in the field of additive manufacturing, which develops the components by building layers, depends upon the proper selection of their optimum input attributes. Components manufacturing as per anticipated size is accomplished by the optimization of factors, namely, heater power (H), layer height (L), the feed rate of the heater (F) and roller (R), and support’s temperature (S) using “Multi-Response Particle Swarm Optimization (MRPSO)”. Analysis of variance was employed to substantiate the competence of the established models. Trials have shown that mechanical properties of manufactured components are characterized by Design of experiments in a direct relationship with F and R, but inversely related to H and L. Finally, unique MRPSO algorithm has been employed for parallel optimization of multiple outputs. Introduced mutation functions (of genetic algorithm) into MRPSO algorithm to prevent early convergence. Optimal-solutions of Pareto-front achieved by MRPSO were graded by the compound grades (resulting from maximum deviation theory) to increase preciseness in making the decisions. The MRPSO analysis offered valuable information for monitoring the factors to improve the accuracy of SIS components. Massive optimal-solution data have been generated for every possible combination of factors to maximize the responses.

Keywords: Selective Inhibition Sintering; Multi-objective Optimization; ANOVA; Mechanical Properties; Additive Manufacturing; MOPSO.

1. Introduction

Innovative manufacturing processes undergo many phases, like innovating a product with an object, qualifying refined idea and designing advanced manufacturing methods. But 3rd phase involves producing intricately shaped parts using “Rapid Prototyping (RPT)” from CAD source files because of its broader application in automotive, biomedical, and aircraft industries for developing operational, trial product and intangible parts. Also, RPT builds complex configurations without using tools and reducing production preparedness time equal to 60% contrasted to existing methods (Hilton et al., 2000). Classification of RPT depends on the processing of materials like “Stereo-Lithography (SLA)”, “Fused Deposition Modeling (FDM)”, and “Laminated Object Modeling (LOM)” for liquid resin, solid filament, sheet form etc., respectively (Mahapatra et al., 2012). “Selective Laser Sintering (SLS)” is one of the current developments of RPT for powder form of materials to produce in large quantity production using high-intensity lasers. High-intensity lasers in production system turn into a costly process, and high-speed sintering process is introduced to eliminate the laser sintering process (Rouholamin et al., 2016). To eliminate laser heating, a unique RPT process employing the infrared heating process for sintering powders called as “Selective Inhibition Sintering (SIS)”. But attaining higher accuracy with minimal wastage would become the uncertainty feature influencing SIS survival. Laser sintered are affected by CO₂ to sinter at anticipated layers (Gibson et al., 1997). SIS is applied on selected thin polymer layers formed by powder and wetted by inhibition liquid on boundaries of the surface such that sintered polymer within and next to the boundaries supports the construction. SIS has shown extensive advantages compared with other methods of the RPT technology such as the abolition of costly heating methods, backing material, tooling arrangement, and is cost-effective in handling various powder materials. Disadvantages of SIS, as a complex process, are requiring high strength and excellent surface quality and geometrical accuracy, which involves being accustomed to working factors and manipulating the strength. SIS method is based on the various interdependent factors, in which some are independent. The component strength based on factors like tessellated model accuracy, the algorithm for slicing, equipment resolution, and powder grains geometry, etc.

(Khoshnevis et al., 2003) was noticed. These factors correspondingly lead to advanced input variables like layer thickness, heater power, and heater feed rate. Using these variables, optimization of “Mechanical Output Characteristics (MOC)” using “Response Surface Methodology (RSM)” has been investigated. Moreover, RSM also evaluated the significance of factors on accuracy. The results were validated to qualify the production of parts with acceptable strength (Baligheid et al., 2018). The work extended using two more factors apart from the above, such as roller feed rate and bed temperature, for optimization of parameters on MOC to produce components with anticipated dimensions using the RSM approach. A face-centered composite block design was utilized to prepare the experimentation plan with three leveled factors of the “Polyamide (PA12)” substance for an innovative SIS technique. Then, verified the fitness of generated models using “Analysis of Variance (ANOVA)”. The microstructure was also used to validate the surface texture in collaboration with sensitivity analysis to assess the factor's effect on MOC at optimal conditions (Baligheid et al., 2019). Making the SIS is an evolving process demands lots of developments in other fields. Accurate dimensions of components and strength mainly depend on particle shape, size, and packing density, which are major concerns of most of the present RP technology.

Literature analysis of SIS technology shows that this field is hardly studied. Only a few studies like RSM investigated the impact of input variables on “Mechanical Properties (MP)”, without even taking the weightage of one response on the others in multi-response optimization. Optimal values of input variables and regression models were obtained. These models' accuracy level was deficient as it does not take process non-linearities and modeling difficulties when compared with the accuracy level of experimental results. To increase the accuracy level and to have many optimal conditions of inputs for varying weights of responses, “Particle Swarm Optimization (PSO)” analysis has been studied for the MPs (storage and loss modulus and $\tan \delta$) of components produced from SIS process. Multi-objective optimization is considered for the six inputs or variables. Multi optimal values of six parameters have been suggested for the designers to use as a reference guide at higher accuracy level more than Genetic algorithms and other methods.

2. Methods and materials

Nylon 12 or PA12 powder having a grain size of 110 μm is widely accepted universal plastic having additive production applications because of its durability, ultimate strength, shock strength, and withstand fracture by stretching itself. By removing the moisture content (heating in glycerol up to 120°C for one hour), grain uniformity will be improved. To produce components, we need to select a suitable inhibit solution (potassium iodide + isopropyl alcohol + water) to accelerate the sintering effect and employ it as an inhibitor in the SIS process. The SIS process is studied by a plan of experimental runs for multi-object optimization that should not be repetitive, time intervening, and costly. Therefore, input variables of the SIS process that play a key role in the component quality and accuracy are selected before ensuing running of experimental trials. From the previous work, operating input factors like heater power (H), heater feed rate (F), layer height (L), roller feed rate (R), and bed/support temperature (B) are freely controllable such that they influence directly the MOC of the SIS produced components. Also, their ranges of operation with the designer decision are tabulated in the Table 1. H and B attribute ranges are adopted using the thermic property of substances dealt with. R and F attributes also impact the precision and trigger the non-uniform sintering. Experiments conducted to investigate the strength must be large in number such that one factor varies, keeping other factor values constant.

Table 1. Working factors of SIS and their range

Varying factors	Units	Values	Fixed factors	Units	Values
Heating power (H)	Watts	25, 35, 45	Printer feed rate	m/s	0.03
Layer height (L)	mm	0.2, 0.3, 0.4	Printer frequency	Hz	400
Heater/ Furnace feed rate (F)	mm/s	6, 8, 10	Printer pressure	Bar	0.5
Roller feed rate (R)	mm/s	170, 210, 250	-	-	-
Bed/support temperature (B)	°C	80, 100	-	-	-

When the number of factors affecting the multiple outputs is bigger, the experiment work

has to be increased to cover the effect of every factor level on each output in the traditional techniques. So, a large number of tests are conducted to include most possible combination of input factors. Sometimes it becomes cumbersome to conduct vast trial runs bearing in mind the period and expenditure used during execution of experiments. For such instances, orthogonal matrix-based experimental planning suggested by Taguchi, taking all factor combinations and their levels for every experiment are recommended (Yunus et al., 2016). Taguchi Design employs various design approaches of system, parametric, and tolerance type. By employing RSM, a multi-response optimization technique was performed to choose the level of factors in the grinding process (Yunus et al., 2020). The correctness and proficiency of an SIS process depend on the suitable implementation of the trial strategy and the adoption of their procedures. In this work, a quadratic regression considering the linear, square, and interaction of factors using ANOVA is applied to convert responses into empirical models of the SIS process (Montgomery et al., 2019), (Myers et al., 2016).

Furthermore, The Central Composite Design of RSM is employed, and optimization carried out. RSM proved a suitable approach by increasing efficiency and product superiority to a certain extent (Aldahdooh et al., 2013), (Acherjee et al., 2012), (Balachandran et al., 2012). Maximum one level of each parameter is obtained corresponding optimum condition, and without taking the role of increasing or decreasing the significance of responses on each other as well as a range of optimum factors level is difficult to get under varying requirements of industries. Therefore, we use the above models from ANOVA as objective functions in the PSO algorithm to obtain a range of optimal values of each parameter using evolving methods to a very accuracy level where the RSM method can never reach. PSO handle easily the factors and their levels without exact range using its natural algorithms but they are keenly selected (refer Table 1.). Factors without proper range is not possible by RSM for examining the MOC in sintering of specimens. In this approach, experiment work generated for five-factor level by grouping as per the “Orthogonal-matrix (OA)” of Taguchi design to examine their effect on shrinkage of components. Table L₆₀ OA is selected for the present study.

2.1. Mechanical Properties using Dynamic Mechanical Analysis

Specimens made up of Nylon 12 powder with inhibitor solution for the above analysis keeping with standards of ASTM D638 (dimension of 13 × 3.2 × 60 mm) were prepared. Firstly, 3D model of sample is imported in STL format and split into many segments for defining contour profile by processing software of machine. It facilitates the inhibitor solution nozzle is placed on those split regions to avoid shrinkage factor at different scale and prepares samples at different combination level of SIS factors. The “Dynamic Mechanical Analysis (DMA)” investigates the different behavior of polymers, namely structural “Storage Modulus (SM)” and visco-elastic “Loss Modulus (LM)” at a fixed frequency of 1 Hz using a three-point bending type test, the average values of moduli are noted down. Totally, 60 tests for various design factors (consisting of one categorical and four contributing factors) with various permutations were accomplished and displayed in Table 2.

Three MP in this study were measured namely, storage modulus (measures load-bearing capacity representing structural elastic strength behavior), loss modulus (heat energy dissipation/cycle representing viscous behavior) and tan δ (measures frequency of load absorbing capacity under varying temperature and is defined by percentage of loss modulus from storage modulus). Using ANOVA, every permissible grouping of factors was linked to responses obtained from experimental values in a mathematical form. In this approach, second-order (quadratic type) regression relationship mathematic models for the experimental outputs were generated, to evaluate the impact of factors on the MP in polynomial form as follows:

$$SM = a_0 + a_1(H) + a_2(L) + a_3(F) + a_4R + a_5(B) + a_{11}(H^2) + a_{22}(L^2) + a_{33}(F^2) + a_{44}(R^2) + a_{55}(B^2) + a_{12}(HL) + a_{13}(HF) + a_{14}(HR) + a_{15}(HB) + a_{23}(LF) + a_{24}(LR) + a_{25}(HB) + a_{34}(FR) + a_{35}(FB) + a_{45}(RB) \quad (1)$$

$$LM = b_0 + b_1(H) + b_2(L) + b_3(F) + b_4R + b_5(B) + b_{11}(H^2) + b_{22}(L^2) + b_{33}(F^2) + b_{44}(R^2) + b_{55}(B^2) + b_{12}(HL) + b_{13}(HF) + b_{14}(HR) + b_{15}(HB) + b_{23}(LF) + b_{24}(LR) + b_{25}(HB) + b_{34}(FR) + b_{35}(FB) + b_{45}(RB) \quad (2)$$

$$\text{Tan}\delta = c_0 + c_1(H) + c_2(L) + c_3(F) + c_4R + c_5(B) + c_{11}(H^2) + c_{22}(L^2) + c_{33}(F^2) + c_{44}(R^2) + c_{55}(B^2) + c_{12}(HL) + c_{13}(HF) + c_{14}(HR) + c_{15}(HB) + c_{23}(LF) + c_{24}(LR) + c_{25}(HB) + c_{34}(FR) + c_{35}(FB) + c_{45}(RB) \quad (3)$$

where a_0 , b_0 and c_0 are the average values of the corresponding outputs, and a_1 to a_{45} , b_1 to b_{45} and c_1 to c_{45} represents the coefficients depends on single, square, as well as the interactive effects of factors of Equation (1) to Equation (3) respectively.

Table 2. Data collected as per the L_{60} orthogonal design matrix of the Taguchi method

Runs	H	L	F	R	B	SM (Pa)	LM (Pa)	Tan δ
1	45	0.4	10	170	100	7030210000	780176100	0.110975
2	35	0.3	10	210	100	8207210000	879681000	0.107184
3	45	0.3	8	210	100	9384210000	1080132900	0.115101
4	25	0.4	6	170	80	2399210000	152862600	0.063714
5	25	0.4	6	250	80	7041210000	837860100	0.118994
6	35	0.3	8	210	100	10099210000	1129164300	0.111807
7	25	0.4	10	170	100	6909210000	788828700	0.114171
8	35	0.2	8	210	100	5083210000	501850800	0.098727
9	45	0.4	10	250	100	6843210000	709513200	0.103681
10	45	0.3	8	210	80	6282210000	693650100	0.110415
11	45	0.4	6	170	80	7954210000	850839000	0.106967
12	45	0.2	10	170	80	5842210000	615776700	0.105401
13	25	0.2	6	250	100	6106210000	646060800	0.105804
14	45	0.2	6	170	80	8757210000	933038700	0.106545
15	25	0.4	10	170	80	7976210000	888333600	0.111373
16	35	0.3	8	210	100	3928210000	395135400	0.100589
17	35	0.3	8	210	80	9197210000	971975400	0.105682
18	25	0.2	10	170	80	4379210000	460029900	0.105049
19	45	0.2	6	250	80	6480210000	670576500	0.103481
20	45	0.2	6	250	100	7327210000	728260500	0.099391
21	35	0.3	8	210	80	7096210000	807576000	0.113804
22	35	0.3	8	170	100	3609210000	327356700	0.0907
23	45	0.4	10	250	80	6436210000	654713400	0.101723
24	25	0.4	6	170	100	7558210000	836418000	0.110664
25	45	0.4	10	170	80	5413210000	622987200	0.115086
26	35	0.3	8	210	80	10693210000	1217132400	0.113823
27	35	0.3	10	210	80	5083210000	585492600	0.115182
28	35	0.3	6	210	80	8119210000	879681000	0.108346
29	25	0.4	6	250	100	7976210000	899870400	0.112819
30	45	0.2	6	170	100	10330210000	1121953800	0.108609
31	35	0.3	8	250	80	6568210000	679805940	0.103499
32	35	0.3	8	210	80	7954210000	888333600	0.111681
33	35	0.3	8	210	80	2729210000	269672700	0.09881
34	45	0.4	6	250	80	6381210000	702302700	0.110058
35	35	0.2	8	210	80	8251210000	925828200	0.112205
36	25	0.3	8	210	80	7712210000	915733500	0.118738
37	25	0.2	6	250	80	8427210000	951786000	0.112942
38	45	0.2	10	170	100	7338210000	755660400	0.102976
39	25	0.2	6	170	100	5842210000	641734500	0.109844
40	35	0.3	8	210	100	9604210000	1044080400	0.108711
41	25	0.2	10	250	100	6139210000	657597600	0.107114
42	35	0.3	8	210	100	8581210000	911407200	0.10621
43	35	0.3	8	210	100	11034210000	1166658900	0.105731
44	35	0.3	8	210	80	7250210000	754218300	0.104027
45	45	0.2	10	250	100	8152210000	853723200	0.104723
46	25	0.2	10	250	80	7976210000	798923400	0.100163
47	35	0.3	8	250	100	8185210000	866702100	0.105886
48	45	0.4	6	170	100	7360210000	806133900	0.109526
49	25	0.2	10	170	100	6887210000	798923400	0.116001
50	35	0.4	8	210	100	10902210000	1243090200	0.114022
51	45	0.2	10	250	80	8669210000	1009470000	0.116443
52	25	0.3	8	210	100	3477210000	379272300	0.109074
53	35	0.4	8	210	80	7789210000	847954800	0.108863
54	25	0.4	10	250	100	4181210000	438398400	0.10485
55	45	0.4	6	250	100	8515210000	956112300	0.112283
56	25	0.2	6	170	80	4291210000	490314000	0.11426
57	25	0.4	10	250	80	7019210000	797481300	0.113614
58	35	0.3	8	210	100	6238210000	618660900	0.099173
59	35	0.3	6	210	100	5479210000	536461200	0.097908
60	35	0.3	8	170	80	8306210000	912849300	0.1099

2.2. Particle Swarm Optimization

PSO algorithm principally presented a natural evolution evaluation technique using a population inspired from the bird's flock and fish behavior by Kennedy and Eberhart in 1995. It involves a simple concept, easy to develop, and quick to converge. Therefore, PSO is gaining considerable popularity and has widespread applications, including job forecasting, electrical control, vibration system, supply chain system, automobile routing, and components replacing check difficulties (Wu et al.,2008), (Mohanty et al., 2016). PSO is initiated with the random sized population and appropriate range of bound values of factors (refer Figure 1.). After evaluating the fitness function, the PSO procedure reiterates the subsequent steps repetitively (Gibson et al.,1997):

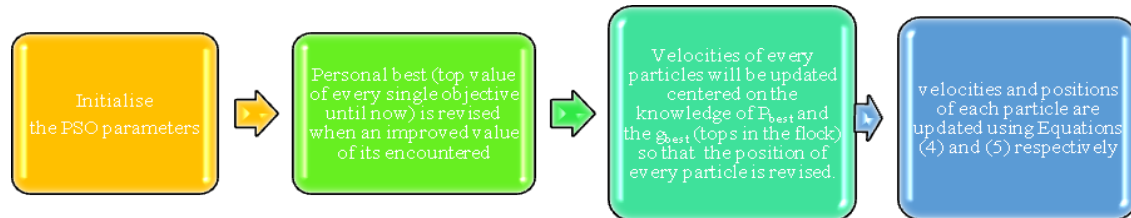


Figure 1. Steps of PSO process

$$v_i(t+1) = wv_i(t) + c_1\text{rand}_1(P_{\text{best}i} - x_i(t)) + c_2\text{rand}_2(G_{\text{best}i} - x_i(t)) \quad (4)$$

$$x_i(t+1) = x_i(t) + v_i(t+1) \quad (5)$$

where $v_i(t)$ and $x_i(t)$ are the velocity and position of an element i at iteration t ; $P_{\text{best}i}$ and $G_{\text{best}i}$ are the personal and global best of particle i ; rand indicates the random number (0 to 1); w is the weighting function; c_1 and c_2 are the cognition and social learning rates; respectively. In the fitness function approach, P_{best} and G_{best} are the personal and general best in each iteration and the group among all personal bests, respectively.

2.3. Proposed Multi-Response Particle Swarm Optimization Algorithm

Present-day problems comprise parallel optimization of various objectives/responses, which are either conflicting or contradicting nature demands “Multi-Response Optimization (MRO)” in most of the applications when responses are two or more. The PSO can also be employed for cracking the MRO problems known as the “Multi-Response Particle Swarm Optimization (MRPSO)” (Tripathi et al.,2007). When every response is considered together, the outcomes are optimum as no supplementary solution within the track region. It means these types of results are outstandingly good to other solutions within track space called as “Pareto-Optimal Solutions (POS)”. The illustration of effective set obtained in the demonstrable space is called a “Non-Dominated (ND)” set because every solution leads the other. ND is identified by comparing and checking the conditions given below. A minimization problem for two objectives can be checked using Equations (6) to (7):

$$\text{Objective}_1[k] > \text{Objective}_1[n] \text{ and } \text{Objective}_2[k] \geq \text{Objective}_2[n] \quad (6)$$

$$\text{or } \text{Objective}_1[k] \geq \text{Objective}_1[n] \text{ and } \text{Objective}_2[k] > \text{Objective}_2[n] \quad (7)$$

where k and n signify output numbers from the population of two objective function values. The MRO has two goals, primarily to converge to the POS set, and secondly to uphold the variety and scatterings in solutions.

In MRO problems, every particle has a g_{best} set (stored in an archive where ND solutions are present), but only one is chosen for updating its position. The MRO keeps the archive updated after every iteration, which was empty at the start and can store a maximum number of user-defined ND solutions. “Crowding Distance (CD)” approach was broadly useful in evolutionary MRO algorithms for promoting multiplicity. CD measure in MROPSO to select g_{best} was first used in (Raquel et al., 2005). The highest number of generations is set as a finishing criterion. Typically, “Multi Factor Decision Making (MFDM/ MADM)” methods are selected to find the

score of the results and for choosing the finest solution, which has the highest grade. But the weights allocated in the MADM process to convert multiple into a single corresponding objective score are practically independent and influence the decision of grading the alternate results greatly. “Maximum-Deviation-Theory (MDT)” proposed for avoiding ambiguity of experts allocating weights and extracting the precise data from the available with the logic of smaller weight given to the responses holding analogous values than the responses holding higher changes/deviations. ND solutions from MROPSO are used for the decision matrix (Yingming et al., 1997). Standardization of every characteristics is performed for altering various scalar values and units amid several characteristics into a joint computable scalar value depending on “larger the better” or “smaller the better” using Equation (8).

$$r_{ij}^* = \frac{r_{ij} - \min_i \{r_{ij}\}}{\max_i \{r_{ij}\} - \min_i \{r_{ij}\}}, \text{ for larger the better characteristics} \quad (8)$$

The ND solutions attained from MROPSO algorithm will be graded by approximating the compound grade of every solution by accumulation of the weighted accomplishment (refer Equation (9)) of all characteristics. \bar{X}_{ij} designates the evaluations of the i^{th} alternative relating to the j^{th} attribute and $d(\bar{X}_{ij}, \bar{X}_{lj})$ indicates the deviation between the two evaluations of i^{th} , l^{th} alternatives relating to the j^{th} attribute. The normalized attribute weights are determined as follows:

$$w_j = \frac{\sum_{i=1}^N \sum_{l=1}^N [(d(\bar{X}_{ij}, \bar{X}_{lj}))]}{\sum_{j=1}^M \sum_{i=1}^N \sum_{l=1}^N [(d(\bar{X}_{ij}, \bar{X}_{lj}))]} \quad (9)$$

3. Result and Discussions

Quadratic or second-order statistical models for the three responses of MP were generated by verifying the adequacy of the models using ANOVA. It considers the effect of interaction along with single, square of factors on different outputs measured by the ANOVA approach of Minitab software to develop mathematical relationships between various MP and factors from Tables 2.

The R-square value of relationship models for SM, LM and Tan δ are 0.80, 0.82 and 0.85 respectively shows the linear relationship which is agreeable and non-linear relationship of 20%, 18%, and 15% between investigational and forecast results is disagreeable. The models for SM, LM, and Tan δ are expressed in Equation (10) to Equation (12), having all defined factors.

$$\begin{aligned} \text{SM} = & -31325231717 + 450366224 \times \text{H} - 53702117599 \times \text{L} + 2881695198 \times \text{F} + 241089992 \times \text{R} - 438472 \times \text{B} \\ & - 4894035 \times \text{H}^2 + 80309649123 \times \text{L}^2 - 120288377 \times \text{F}^2 - 335096 \times \text{R}^2 - 249218750 \times \text{H} \times \text{L} - 14385938 \times \text{H} \times \text{F} \\ & - 769141 \times \text{H} \times \text{R} + 3391667 \times \text{H} \times \text{B} - 187343750 \times \text{L} \times \text{F} - 29820312 \times \text{L} \times \text{R} + 242611111 \times \text{L} \times \text{B} - 47266 \times \text{F} \times \text{R} \\ & - 5209722 \times \text{F} \times \text{B} - 633264 \times \text{R} \times \text{B} \end{aligned} \quad (10)$$

Model-predicted for SM includes all linear, square, and interaction terms with positive and negative signs. Equation (10) indicates that linear terms like H, F and R along with Bed temperature, and interaction terms of H, B, and L have an positive impact on SM.

$$\begin{aligned} \text{LM} = & -4288599167 + 25581488 \times \text{H} - 7353436171 \times \text{L} + 395054038 \times \text{F} + 36654368 \times \text{R} + 2535733 \times \text{B} \\ & - 174406 \times \text{H}^2 + 9504324500 \times \text{L}^2 - 16077201 \times \text{F}^2 - 54975 \times \text{R}^2 - 25011422 \times \text{H} \times \text{L} - 1466886 \times \text{H} \times \text{F} \\ & - 91596 \times \text{H} \times \text{R} + 345703 \times \text{H} \times \text{B} - 20054203 \times \text{L} \times \text{F} - 1791359 \times \text{L} \times \text{R} + 34810692 \times \text{L} \times \text{B} - 136887 \times \\ & \times \text{F} \times \text{R} - 658960 \times \text{F} \times \text{B} - 88669 \times \text{R} \times \text{B} \end{aligned} \quad (11)$$

The generated statistical model for the loss modulus (refer to equation (11)) shows that F, R, and B have positive and heater power and layer height have a negative effect on LM, the square effect of heater power has positive as well as the interaction of H, L and B factors have a positive effect on LM.

$$\begin{aligned} \text{Tan} \delta = & -0.106 - 0.00232 \times \text{H} - 0.380 \times \text{L} + 0.0129 \times \text{F} + 0.00201 \times \text{R} + 0.00103 \times \text{B} + 0.000056 \times \text{H}^2 + 0.068 \times \text{L}^2 \\ & - 0.000156 \times \text{F}^2 - 0.000003 \times \text{R}^2 + 0.00137 \times \text{H} \times \text{L} - 0.000030 \times \text{H} \times \text{F} - 0.000004 \times \text{H} \times \text{R} - 0.000011 \times \text{H} \times \text{B} \\ & + 0.00523 \times \text{L} \times \text{F} + 0.000423 \times \text{L} \times \text{R} + 0.00183 \times \text{L} \times \text{B} - 0.000029 \times \text{F} \times \text{R} - 0.000047 \times \text{F} \times \text{B} - 4 \times 10^{-6} \times \text{R} \times \text{B} \end{aligned} \quad (12)$$

Equation (12) shows that linear terms like F, R, and B and interaction terms like H as well as F, B, and L have a positive effect. The impact of selected SIS factors such as H, L, F, R and B on

dynamic MP of Nylon 12 samples depends on the understanding of P-value of ANOVA for designated working factors on MPs.

Table 3. ANOVA results of Storage Modulus

Basis	Degree of Freedom	Adjusted Sum of Squares	Adjusted Mean Squares	F-value	P-value
Model	19	4.70668E+19	2.47720E+18	0.56	0.912
Linear	5	1.91773E+19	3.83545E+18	0.87	0.511
H	1	1.36875E+19	1.36875E+19	3.10	0.086
L	1	9.80100E+15	9.80100E+15	0.00	0.963
F	1	9.54855E+17	9.54855E+17	0.22	0.645
R	1	2.91328E+18	2.91328E+18	0.66	0.422
B	1	1.61179E+18	1.61179E+18	0.36	0.549
Square	4	1.07626E+19	2.69064E+18	0.61	0.659
H*H	1	1.24113E+18	1.24113E+18	0.28	0.599
L*L	1	3.34209E+18	3.34209E+18	0.76	0.390
F*F	1	1.19964E+18	1.19964E+18	0.27	0.605
R*R	1	1.48957E+18	1.48957E+18	0.34	0.565
2-Way Interaction	10	1.71270E+19	1.71270E+18	0.39	0.945
H*L	1	1.98752E+18	1.98752E+18	0.45	0.506
H*F	1	2.64903E+18	2.64903E+18	0.60	0.443
H*R	1	3.02888E+18	3.02888E+18	0.69	0.413
H*B	1	4.14123E+18	4.14123E+18	0.94	0.339
L*F	1	4.49250E+16	4.49250E+16	0.01	0.920
L*R	1	4.55297E+17	4.55297E+17	0.10	0.750
L*B	1	2.11897E+18	2.11897E+18	0.48	0.493
F*R	1	4.57531E+14	4.57531E+14	0.00	0.992
F*B	1	3.90833E+17	3.90833E+17	0.09	0.768
R*B	1	2.30989E+18	2.30989E+18	0.52	0.474
Error	40	1.76866E+20	4.42166E+18		
Lack-of-Fit	30	1.04758E+20	3.49193E+18	0.48	0.939
Pure Error	10	7.21084E+19	7.21084E+18		
Total	59	2.23933E+20			
R-sq		80.02%			
Adj. R-squared		79.17			
Pred. R-squared		81.16			

Table 4. ANOVA results of Loss Modulus

Basis	Degree of Freedom	Adjusted Sum of Squares	Adjusted Mean Squares	F-value	P-value
Model	19	5.58278E+17	2.93831E+16	0.46	0.965
Linear	5	1.80761E+17	3.61521E+16	0.56	0.727
H	1	1.30152E+17	1.30152E+17	2.03	0.162
L	1	1.76915E+15	1.76915E+15	0.03	0.869
F	1	8.29787E+15	8.29787E+15	0.13	0.721
R	1	3.20972E+16	3.20972E+16	0.50	0.483
B	1	8.44481E+15	8.44481E+15	0.13	0.718
Square	4	1.42818E+17	3.57046E+16	0.56	0.695
H*H	1	1.57617E+15	1.57617E+15	0.02	0.876
L*L	1	4.68085E+16	4.68085E+16	0.73	0.398
F*F	1	2.14300E+16	2.14300E+16	0.33	0.566
R*R	1	4.00908E+16	4.00908E+16	0.63	0.434
2-Way Interaction	10	2.34699E+17	2.34699E+16	0.37	0.954
H*L	1	2.00183E+16	2.00183E+16	0.31	0.579
H*F	1	2.75425E+16	2.75425E+16	0.43	0.516
H*R	1	4.29558E+16	4.29558E+16	0.67	0.418
H*B	1	4.30239E+16	4.30239E+16	0.67	0.417
L*F	1	5.14779E+14	5.14779E+14	0.01	0.929
L*R	1	1.64299E+15	1.64299E+15	0.03	0.874
L*B	1	4.36242E+16	4.36242E+16	0.68	0.414
F*R	1	3.83754E+15	3.83754E+15	0.06	0.808

F*B	1	6.25288E+15	6.25288E+15	0.10	0.756
R*B	1	4.52863E+16	4.52863E+16	0.71	0.406
Error	40	2.56309E+18	6.40774E+16		
Lack-of-Fit	30	1.59477E+18	5.31591E+16	0.55	0.900
Pure Error	10	9.68321E+17	9.68321E+16		
Total	59	3.12137E+18			
R-squared		81.04%			
Adj. R-squared		85.97			
Pred. R-squared		71.16			

Table 5. ANOVA results of Tan δ

Basis	Degree of Freedom	Adjusted Sum of Squares	Adjusted Mean Squares	F-value	P-value
Model	19	0.001071	0.000056	0.80	0.692
Linear	5	0.000099	0.000020	0.28	0.920
H	1	0.000001	0.000001	0.01	0.909
L	1	0.000005	0.000005	0.07	0.787
F	1	0.000053	0.000053	0.75	0.392
R	1	0.000018	0.000018	0.26	0.612
B	1	0.000022	0.000022	0.32	0.577
Square	4	0.000239	0.000060	0.85	0.501
H*H	1	0.000160	0.000160	2.27	0.139
L*L	1	0.000002	0.000002	0.03	0.856
F*F	1	0.000002	0.000002	0.03	0.866
R*R	1	0.000145	0.000145	2.06	0.159
2-Way Interaction	10	0.000732	0.000073	1.04	0.428
H*L	1	0.000060	0.000060	0.85	0.362
H*F	1	0.000011	0.000011	0.16	0.689
H*R	1	0.000065	0.000065	0.92	0.343
H*B	1	0.000045	0.000045	0.64	0.427
L*F	1	0.000035	0.000035	0.50	0.485
L*R	1	0.000092	0.000092	1.30	0.260
L*B	1	0.000121	0.000121	1.72	0.198
F*R	1	0.000173	0.000173	2.46	0.125
F*B	1	0.000032	0.000032	0.45	0.504
R*B	1	0.000098	0.000098	1.40	0.244
Error	40	0.002812	0.000070		
Lack-of-Fit	30	0.002510	0.000084	2.78	0.046
Pure Error	10	0.000301	0.000030		
Total	59	0.003882			
R-squared		81.04%			
Adj. R-squared		76.97%			
Pred. R-squared		81.23%			

Heater power (H) showing a substantial effect on the MP of Selective Inhibitor Sintering process is achieved. An increase of H (from 25 to 45W) increases the heat transmission into powdered nylon bed resulting into the quick melting of it placed at inhibitor. But inhibitor region shortens the flow of nylon12 particles which are rushing in it and instead of flowing inside, the molten nylon 12 flows out. Melting of the powder at inhibition influence the component's accuracy decreases the MP because of the over melting of polymer powder. Parts produced with lower H = 25 W exhibits suitable sintering characteristics, and density improves MP. The factor F shown the nominal impact on LM and tan δ because increasing F resulted in the very small change in mechanical properties. The factor R also showed the nominal impact of it on SM, LM, and tan δ when R varied (from 170 to 250 mm/s). But higher feed rates increase the densification of powder result in improved MP. Bed temperature (B) was not found affecting MP. Still, this factor plays a role in heating bed or support below the melting point of nylon powder during sintering for reducing thermal alteration to initiate fusion between consecutive layers. Increasing B lessens the cooling rate. The strength and density of the components found useful at maximum value of B (Kruth et al., 2004).

The experimental responses showed that the selected factors were exhibiting a significant role in

MP of components produced using the SIS process. The next step is the optimization of factors for finding the optimal set of working factors to fabricate the components with the enhanced dynamic MP. Predicted factors levels of H, L, F, R, and B improve the dynamic MP (SM, LM, and Tan δ).

3.1. MROPSO Analysis results

Three outputs, such as SM, LM, and Tan δ, were considered in this study. However, all three objectives cannot be valid concurrently for manufacturing products. The selection of outputs are solely governed by the need of a design engineer. So, two outputs at a time will be optimized considering the third one as constraint. Third output controlled value is taken from the experimental inspections. The objective function required for MROPSO is provided by an empirical model obtained between the factors and outputs developed from the ANOVA to solve the optimization of the problem. In the current work, all the objectives (SM, LM, and Tan δ) are to be maximized, which are the functions of factors H, L, F, R, and B. Hence, the objective functions SM, LM and Tanδ are switched into minimization mode and the objective functions are altered as below:

Objective 1= Minimize (1/SM) = - (SM);

Objective 2= Minimize (1/LM) = - (LM);

Objective 3= Minimize (1/Tanδ) = - (Tanδ).

Three optimization problems were designed considering two outputs as objectives and the third one as a constraint. The empirical models from Equation (10) to Equation (12) were used as functional relationships in MROPSO coded in MATLAB® R20 for solving the following minimization cases.

Case 1: Maximizing SM and LM subjected to $Tan \delta \geq 0.1189946$ is the highest value acquired from experimentation (refer to Table 2).

Case 2: Maximizing SM and Tan δ subjected to $LM \geq 1243090200$ is the maximum value from the experimentation (refer to Table 2).

Case 3: Maximizing the LM and Tan δ subjected to $SM \geq 11034210000$ is the highest value acquired from the experimentation (refer Table 2).

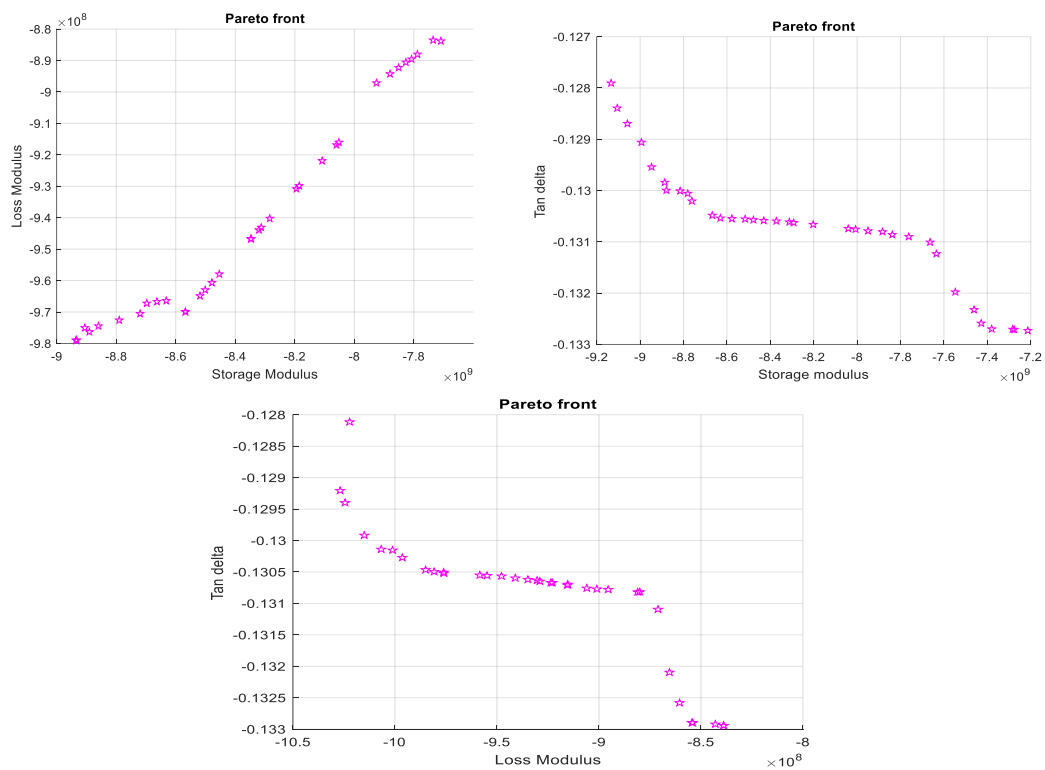


Figure 2. Pareto front for objectives: (a) SM and LM (b) SM and Tan δ (c) LM and Tan δ

Instead of maximization of the objective, an equivalent/consistent minimization function is to be utilized in the MATLAB program by using -ve sign. Simulation is performed to establish the capability of the MROPSO algorithm. The initial population was set to 100 for the present algorithm. The factors applied to MROPSO such as the initial population size =100, the inertia weight= $0.5(\text{rand}+1)/2$, and both the $c_1 = c_2 = 1.5$ (cognitive and social factor). This developed three sets of Pareto-fronts viz. SM and LM, SM, and Tan δ and LM and Tan δ were generating an optimal solution for the outputs.

Table 6. Pareto optimal solution for SM and LM

V	H	L	F	R	B	SM	LM
1	44.9999	0.39996	9.04575	211.015	81.967	5924708534.4	723844445.2
2	42.8275	0.20091	6.0417	207.351	99.995	9130128036.5	1011656247.2
3	44.9804	0.39994	6.61465	210.051	93.073	8067534579.9	960660497.6
4	44.9486	0.399995	6.00953	206.309	99.999	8859230241.1	1042880230.2
5	44.9820	0.39996	6.33328	207.885	99.293	8715615682	1029274430.4
6	44.9887	0.39995	7.33068	210.679	85.554	7192003725	868714981.6
7	44.9889	0.39996	6.58807	208.858	96.921	8429981472.9	999562296
8	44.9950	0.39995	7.0801	210.755	88.883	7561440353.2	907810531
9	44.9986	0.39995	8.6477	211.015	81.969	6211135912.1	758448627
10	44.9965	0.39989	7.4896	210.865	83.447	6950748308	843105766
11	44.9991	0.39994	8.8882	211.018	82.007	6045551551	738441940.3
12	44.9913	0.39995	7.4464	210.937	85.458	7136826018	862677927.6
13	43.3957	0.2185	6.0427	206.519	99.999	8864161585.3	988913394
14	44.9998	0.39997	8.7743	211.013	81.98	6124977428.7	748088085.6
15	43.3529	0.20264	6.2368	208.202	98.62	9022837871.6	1007553740.8
16	44.9926	0.39995	7.2487	210.841	82.688	6977073963.7	846167762.6
17	44.9932	0.39996	7.0318	210.919	97.350	8302189915.8	985901736
18	44.9887	0.39989	7.2854	209.465	86.207	7273473843.7	877613601.7
19	44.9997	0.39996	8.4621	211.004	82.081	6340261047.3	773756145
20	44.9988	0.39996	8.5549	211.004	82.030	6277244457.7	766292593.6
21	44.9971	0.39997	6.8887	210.736	90.922	7796964770.9	932573507.1
22	44.9999	0.39995	7.0801	210.763	88.883	7560768645.4	907785426.5
23	44.9902	0.39995	7.07	209.713	90.643	7727176086.8	925554980.6
24	44.9950	0.39993	7.0483	210.795	86.613	7376508905.4	888267890.7
25	44.9959	0.39996	7.0195	209.4191	92.466	7904323642.1	944422747.2
26	44.9992	0.39993	6.811	210.957	93.085	8004065603.2	954305590
27	44.9592	0.39999	6.5726	207.315	97.518	8510339407.9	1008248563.1
28	44.9918	0.39996	6.4687	207.989	99.107	8666798648.7	1024699181.8
29	44.9973	0.39998	6.8113	210.333	89.060	7661032431.3	918165668.9
30	44.9955	0.39995	7.756	210.804	82.129	6728780903.4	819033814.6
31	44.9973	0.39995	8.1996	210.929	82.168	6504226679.7	793027808.8
32	44.9969	0.39996	7.9227	210.997	82.120	6646994296.7	809666608.4
33	44.9963	0.39996	6.7059	209.121	94.229	8156384944	970782177.4
34	42.8426	0.20091	6.0418	207.36	99.980	9129536399.7	1011735225.61
35	44.9748	0.39997	7.2670	210.345	88.407	7462124682.6	897183174.75

Table 7. Pareto optimal solution for SM and Tan δ

No.	H	L	F	R	B	SM	Tan δ
1	44.965	0.39998	7.0713	203.464	99.975	9164652577.07	0.128090
2	26.421	0.3998	7.983	224.035	99.939	7753792890.24	0.13065
3	25.008	0.39996	8.7997	233.248	99.923	7395642921.71	0.133078
4	44.998	0.39996	7.4594	231.285	98.301	8599420961.33	0.1306331
5	44.259	0.39995	6.859	203.302	99.998	9178155159.79	0.127097
6	25.872	0.39995	8.118	232.552	99.808	7609447790.06	0.131897
7	25.021	0.39995	8.630	232.579	99.832	7435574124.03	0.13302
8	44.995	0.39992	7.374	231.533	99.653	8692620834.61	0.130621
9	44.997	0.39991	7.472	231.673	97.811	8556669684.47	0.130635
10	26.171	0.39979	7.983	224.160	99.939	7716903120.15	0.130928
11	44.975	0.39995	7.371	226.436	99.834	8820357132	0.130538
12	44.963	0.39991	7.165	215.775	99.902	9032787997.85	0.129806
13	44.967	0.39989	7.163	217.011	99.707	9000666790.63	0.129912
14	44.997	0.39991	7.472	231.548	97.811	8559539904.75	0.13064

15	25.008	0.39996	8.7998	233.248	99.923	7395642921.71	0.133078
16	25.570	0.39991	8.3592	227.457	99.822	7590061639.38	0.13202
17	44.978	0.39992	7.1304	219.824	99.918	8976206045.61	0.13016
18	25.185	0.39979	8.2242	230.000	99.948	7523698616.22	0.132621
19	44.996	0.39996	7.4314	230.694	98.919	8657179152.30	0.13063
20	26.683	0.39983	8.0629	227.245	99.914	7768727921.27	0.13069
21	44.987	0.39992	7.4256	220.628	99.765	8915692118.92	0.1302997
22	26.114	0.39986	8.110	226.893	99.816	7689751140.07	0.131269
23	44.977	0.39994	7.354	228.609	99.661	8764367758.94	0.130584
24	44.953	0.39991	7.1299	213.046	99.832	9065435409.14	0.129483
25	44.982	0.39994	7.4082	221.923	99.797	8898652126.39	0.13037
26	25.649	0.39995	8.2951	232.471	99.774	7567001991.38	0.13219
27	44.991	0.39995	7.3739	223.126	99.684	8874086796.99	0.13043
28	44.968	0.39996	7.0978	221.67	99.87	8944987609.83	0.13026
29	44.9955	0.399951	7.4231	231.452	99.201	8658742182.09	0.130624
30	44.951	0.39977	7.1135	208.757	99.801	9106268948.89	0.12891
31	44.993	0.39995	7.3534	230.197	99.656	8727879798.19	0.13062
32	25.234	0.3998	8.3649	233.002	99.787	7493506107.19	0.13272
33	44.977	0.3999	7.2290	228.359	99.661	8785426350.75	0.13057
34	25.008	0.3999	8.5498	233.498	99.923	7435988478.47	0.133067
35	26.683	0.3998	8.3129	226.995	99.914	7751000127	0.130758

Table 8. Pareto optimal solution for LM and Tan δ

No.	H	L	F	R	B	Tan δ	LM
1	25.0002	0.3999997	8.6996	235.46	99.996	0.133141	846014347.03
2	44.9939	0.399996	6.9805	215.02	99.996	0.12969	1024981380.7
3	44.9982	0.399991	8.5487	230.59	89.47	0.13095	882589439.71
4	44.9967	0.399998	7.4075	229.78	99.397	0.13062	981396856.3
5	43.5309	0.399989	6.8444	214.74	99.998	0.12808	1017647892.2
6	44.9966	0.399978	8.4348	230.30	89.65	0.130933	889229745.75
7	44.995	0.399957	8.0974	229.43	91.82	0.13079	917103039.78
8	25.282	0.399976	8.2978	232.72	99.85	0.132648	862488559.63
9	44.996	0.399988	7.3087	228.38	99.472	0.130598	987585226.18
10	44.988	0.399964	7.688	229.79	94.056	0.130668	940968133.93
11	44.9968	0.399972	8.1541	229.92	93.266	0.130748	923026404.8
12	44.994	0.399995	7.2976	218.46	99.859	0.130128	1016207836.7
13	44.994	0.399988	7.2032	216.10	99.637	0.129875	1019656895
14	25.178	0.399443	8.6110	235.43	99.989	0.132893	848279975.4
15	44.996	0.399979	7.4335	229.87	97.669	0.130623	969031585.1
16	44.994	0.399977	7.1800	222.04	99.825	0.130334	100878918.4
17	25.089	0.399999	8.1579	232.05	99.992	0.132847	863863284.69
18	26.037	0.399959	8.0292	229.97	97.683	0.131165	876796307.01
19	44.993	0.399995	7.3196	222.71	99.503	0.130395	1003609192.5
20	44.995	0.399986	7.2452	226.73	99.781	0.130556	995370378.9
21	44.997	0.399979	8.2831	230.30	89.671	0.130911	895225089.2
22	44.984	0.399943	8.1605	230.30	90.050	0.130858	901712593.5
23	26.181	0.399851	7.884	228.77	98.524	0.131002	879765304.6
24	44.996	0.399977	7.5011	229.90	95.957	0.130637	956484234.7
25	44.997	0.399975	8.0347	229.96	94.163	0.130714	932442677.2
26	44.996	0.399983	7.8994	230.21	91.909	0.130764	921182596.
27	44.997	0.399994	7.259	229.09	99.476	0.130609	985909428.1
28	44.986	0.39996	8.1302	229.64	91.544	0.130789	913758653.7
29	44.997	0.399984	8.4348	230.26	89.822	0.130924	890424248.2
30	44.997	0.399996	7.6603	230.22	96.011	0.130657	953127216.2
31	44.987	0.399995	7.3208	223.95	99.452	0.130447	1000008964.9
32	25.431	0.399933	8.2685	231.1	98.285	0.132122	868067951
33	25.781	0.399742	8.0653	230.42	99.799	0.131864	872679574
34	44.999	0.39998	7.5751	229.75	97.057	0.13064	963074843.1
35	44.996	0.39998	7.5439	229.7	97.089	0.13063	963809808.8

Table 9. Best ND solution for three cases

No.	H	L	F	R	B	SM	Objective values		Normalized objective	Weighted normalized		Composite score			
							LM	Tan δ							
1	42.8275	0.20091	6.0417	207.351	99.995	9130128036.5	1011656247.2	0.1299	1	0.5224	0.1406	0.4	0.2089	0.028	0.6369
2	44.963	0.39991	7.165	215.775	99.902	9032787997.85	1022302908.3	0.129810.6517	1	0	0.2607	0.4	0		0.6607
3	44.987	0.399995	7.3208	223.95	99.452	8850622722.4	1000008964.9	0.13045	0	0	1	0	0	0.2	0.2

Figure 2 (a), (b), and (c) show the Pareto-front for SM and LM, SM and $\tan \delta$, and LM and $\tan \delta$, respectively, and a corresponding sample set of the optimal solutions have been provided in Table 6, 7 and 8. Yet, usage of MROPSO yields in a huge number of ND solutions for improving the grouping of objectives of MPs viz. SM-LM, SM- $\tan \delta$, and LM- $\tan \delta$. The different results of the Pareto front achieved from MROPSO were graded by the composite scores of MDT for selecting the finest solution. The decision matrix is standardized/normalized using Equation 8 accurately with the “Objective Weights (OW)” that were established for the “Standardized Output (SO)” values by employing the MDT by means of Equation 9. They are converted into “Weighted Objective Functional (WOF)” values by multiplication of the SO values and the OW. The optimum solution is nominated on the basis of their composite scores obtained by the adding all the WOF values of every alternative. The outputs having the maximum combined score are preferred as the finest solution. Table 9 showing the top-graded solution for various grouping of many outputs.

4. Conclusions

The study presented a joint technique of ANOVA allied with multi-response PSO for the optimization of the mechanical properties of SIS manufacturing process on Nylon 12 material. Secondly, MDT of OW estimation was conducted to evaluate the weights of the factors. The compound grade for all the ND solutions was determined by the summation of the WO values. The finest solution is chosen by considering the maximum out of all ND solution to increase objectiveness and preciseness in the decision making for the inspectors. This investigation provides an operative guide to select optimal factor settings for achieving the desired MP of the SIS process to the instructor and experts. From the data of experiments sections and exploration, the following inferences can be drawn:

1. Higher the Heater power (H) showed the MP decreasing, but the optimum value is contributing to maintaining the maximum MP.
2. The increase of layer height also decreasing the MP, and its minimum value is preferred due to the density variation of components at their higher layer heights.
3. The increasing effect of F found not affecting SM but nominally increased LM and $\tan \delta$. Factor R also has shown a nominal rise in the MP.
4. Factor B did not show any role in MP in experiments, but its value is adopted by MROPSO analysis.
5. From MROPSO, all factors at their different levels presented their corresponding responses as a pool of many solutions, which covers the various levels of factors to maximize the responses as a hand guide to design and production engineers. Pareto front solutions for three responses using MDT, it is inferred that best solution is having factor set of $H = 42.8275$ W, $L = 0.20091$ μm , $F = 6.0417$ mm/s, $R = 207.351$ mm/s and $B = 99.995^\circ\text{C}$ produce very improved MP to higher accuracy level.
6. From MROPSO results, it is also seen. B is the most insignificant factor as B remains the same for most of the optimal solutions to maximize the responses.

REFERENCES

1. Acherjee, B., Kuar A.S., Mitra S., Misra D. (2012). *Modeling and analysis of simultaneous laser transmission welding of polycarbonates using an FEM and RSM combined approach*. Optics & Laser Technology, 2012. 44(4): pp. 995-1006.
2. Aldahdooh, M.A.A., N. Muhamad Bunnori, Megat Johari, M.A. (2013). *Evaluation of ultra-high-performance-fiber reinforced concrete binder content using the response surface method*. Materials & Design (1980-2015), 2013. 52: pp. 957-965.
3. Balachandran, M., Sriram, D., Muraleekrishnan, R., Bhagawan, S.S. (2012). *Optimizing properties of nanoclay–nitrile rubber (NBR) composites using Face Centred Central Composite Design*. Materials & Design, 2012. 35: pp. 854-862.
4. Baligheid, S.M., Chandrasekhar, U., Elangovan, K., Shankar, S. (2018). *RSM Optimization of Parameters influencing Mechanical properties in Selective Inhibition Sintering*. Materials Today: Proceedings, 2018. 5(2, Part 1): p. 4903-4910.
5. Baligheid, S.M., Chandrasekhar, U., Elangovan, K., Shanka, S. (2019). *Investigation of parameters influencing mechanical properties in SIS by using RSM*. International Journal of Materials and Product Technology, 2019. 58(2/3): pp. 178-200.
6. Gibson, I., D. Shi (1997). *Material properties and fabrication parameters in selective laser sintering process*. Rapid Prototyping Journal, 1997. 3(4): pp. 129-136.
7. Hilton, P.D., Jacobs, P. (2000). *Rapid Tooling: Technologies and Industrial Applications*. 1 edition ed. 2000, Marcel Dekker, New York: CRC Press.
8. Khoshnevis, B., Asiabanpour, B., Mojdeh M. (2003). *SIS – a new SFF method based on powder sintering*. Rapid Prototyping Journal, 2003. 9(1): pp. 30-36.
9. Kruth, J.P., Froyen, L., Van Vaerenbergh, J., Mercelis, P., Rombouts, M., Lauwers, B. (2004). *Selective laser melting of iron-based powder*. Journal of Materials Processing Technology, 2004. 149(1): pp. 616-622.
10. Mahapatra, S.S., Sood, A.K. (2012). *Bayesian regularization-based Levenberg–Marquardt neural model combined with BFOA for improving surface finish of FDM processed part*. The International Journal of Advanced Manufacturing Technology, 2012. 60(9): pp. 1223-1235.
11. Mohanty, C.P., S.S. Mahapatra, Singh, M.R. (2016). *A particle swarm approach for multi-objective optimization of electrical discharge machining process*. Journal of Intelligent Manufacturing, 2016. 27(6): pp. 1171-1190.
12. Montgomery, D.C. (2019). *Design and Analysis of Experiment*. 10th ed. 2019, USA: Wiley.
13. Myers, R.H., D.C. Montgomery, Anderson-Cook, C.M. (2006). *Response Surface Methodology: Process and Product Optimization Using Designed Experiments*. 3rd ed. 2016, USA: John Wiley & Sons.
14. Raquel, C.R., Naval, P.C. (2005). *An effective use of crowding distance in multiobjective particle swarm optimization*. In Proceedings of the 7th annual conference on Genetic and evolutionary computation. 2005, Association for Computing Machinery: Washington DC, USA. pp. 257–264.
15. Rouholamin, D., Hopkinson, N. (2016). *Understanding the efficacy of micro-CT to analyse high speed sintering parts*. Rapid Prototyping Journal, 2016. 22(1): pp. 152-161.
16. Tripathi, P.K., S. Bandyopadhyay, Pal, S.K. (2007). *Multi-Objective Particle Swarm Optimization with time variant inertia and acceleration coefficients*. Information Sciences, 2007. 177(22): pp. 5033-5049.

17. Wu, C.-H., Wang, D.-Z., Ip, A., Wang, D.-W., Chan, C.-Y., Wang, H.-F. (2009). *A particle swarm optimization approach for components placement inspection on printed circuit boards*. Journal of Intelligent Manufacturing, 2009. 20(5): pp. 535-549.
18. Yingming, W. (1997). *Using the method of maximizing deviation to make decision for multiindices*. Journal of Systems Engineering and Electronics, 1997. 8(3): pp. 21-26.
19. Yunus, M., Alsoufi, M.S. (2016). *Experimental investigations on precision machining of thermal barrier coatings and application of the grey relation approach to determine the optimum process parameters*. High Temperature Material Processes, 2016. 20(4): pp. 333-354.
20. Yunus, M., Alsoufi, M.S. (2020). *Application of Response Surface Methodology for the Optimization of the Control Factors of Abrasive Flow Machining of Multiple Holes in Zinc and Al/SiCp MMC Wires*. Journal of Engineering Science and Technology, 2020. 15(1): pp.655-674.



Mohammed YUNUS is Associate Professor (since 2014) in the Department of Mechanical Engineering, College of Engineering and Islamic Architecture, Makkah, Kingdom of Saudi Arabia. He graduated from the Faculty of Mechanical Engineering, Gulbarga University, India (1997), and he has a master's degree in Machine design – Visvesvaraya Technological University, India (2000) and also has a PhD. Doctoral degree in Manufacturing, Thermal and Design - Anna University, Chennai, India (2012). The main areas of interest for the research activity include: Thermal Barrier Coatings, Composites, CAE, CFD, HVAC, Smart materials, CIM, Aerospace Components Couplings, Surface Characterization, Solid Mechanics, Fluid Mechanics, Optimization and Genetic Algorithm, renewable energy sources, water treatment, Compliant Mechanisms etc.



Mohammad S. ALSOUFI has received the BSc degree in Mechanical Engineering from Umm Al-Qura University in 2004, and he received the MSc and Ph.D. in Advanced Mechanical Engineering from Warwick University in the United Kingdom in 2007 and 2011, respectively. Now, he is working as a professor in the Mechanical Engineering Department, at Umm Al-Qura University.